Doppler Cloud Radar Derived Drop Size Distributions in Liquid Water Stratus Clouds

SEIJI KATO

Center for Atmospheric Sciences, Hampton University, Hampton, Virginia

GERALD G. MACE

Department of Meteorology, University of Utah, Salt Lake City, Utah

EUGENE E. CLOTHIAUX

Department of Meteorology, The Pennsylvania State University, University Park, Pennsylvania

JAMES C. LILJEGREN

Argonne National Laboratory, Argonne, Illinois

RICHARD T. AUSTIN

Department of Atmospheric Science, Colorado State University, Fort Collins, Colorado

(Manuscript received 7 February 2000, in final form 22 August 2000)

ABSTRACT

A cloud particle size retrieval algorithm that uses radar reflectivity factor and Doppler velocity obtained by a 35-GHz Doppler radar and liquid water path estimated from microwave radiometer radiance measurements is developed to infer the size distribution of stratus cloud particles. Assuming a constant, but unknown, number concentration with height, the algorithm retrieves the number concentration and vertical profiles of liquid water content and particle effective radius. A novel aspect of the retrieval is that it depends upon an estimated particle median radius vertical profile that is derived from a statistical model that relates size to variations in particle vertical velocity; the model posits that the median particle radius is proportional to the fourth root of the particle velocity variance if the radii of particles in a parcel of zero vertical velocity is neglected. The performance of the retrieval is evaluated using data from two stratus case study days 1.5 and 8.0 h in temporal extent. Aircraft in situ microphysical measurements were available on one of the two days and the retrieved number concentrations and effective radii are consistent with them. The retrieved liquid water content and effective radius increase with height for both stratus cases, which agree with earlier studies. Error analyses suggest that the error in the liquid water content vanishes and the magnitudes of the fractional error in the effective radius and shortwave extinction coefficient computed from retrieved cloud particle size distributions are half of the magnitudes of the fractional error in the estimated cloud particle median radius if the fractional error in the median radius is constant with height.

1. Introduction

Interaction of radiation with clouds depends, in part, on the size distribution of the cloud particles. For example, Wiscombe et al. (1984) show that absorption of shortwave radiation increases with the size of cloud particles. For infinitely thick clouds, Twomey and Bohren (1980) show that absorption in the shortwave by cloud is approximately proportional to the square root of the mean radius of cloud particles. Scattering by cloud particles is not negligible in computing radiation in the 8–13-μm wavelength region through clouds (Toon et al. 1989). The intercomparison of radiative transfer models by Ellingson et al. (1991) and a study by Fu et al. (1997) also indicate that the computed infrared irradiance depends on the treatment of scattering by cloud particles.

Some earlier studies demonstrate that the size distribution of stratus cloud particles can be retrieved using radar reflectivity factor from millimeter-wave cloud radar and liquid water path estimated from microwave radiometer radiance measurements (White et al. 1991; Frisch et al. 1995, 1998; Sassen et al. 1999). These algorithms generally assume a specific three-parameter distribution for cloud particles such as a lognormal dis-

Corresponding author address: Seiji Kato, Mail Stop 420, NASA Langley Research Center, Hampton, VA 23681-2199.
E-mail: s.kato@larc.nasa.gov

tribution. Assuming a known value for the geometric standard deviation and taking the number concentration to be constant with height, the algorithms retrieve the liquid water content at each radar sample volume. They derive the number concentration by integrating the liquid water content and matching it with the liquid water path obtained from a microwave radiometer. Given both retrieved liquid water content and number concentration, as well as the estimated geometric standard deviation for each radar sample volume, any moment of the three-parameter particle size distribution can be computed.

One source of error in these retrievals is the use of a climatological value for the geometric standard deviation (Miles et al. 2000). In many retrievals the retrieved size distribution is sensitive to the geometric standard deviation. Hence, if the climatological value assumed for the geometric standard deviation is not close to the actual stratus cloud value, there will be significant error in the retrieval.

This paper discusses an alternative retrieval method that incorporates the median radius of the cloud particle number concentration (count median radius; see Hinds 1982), as opposed to the geometric standard deviation. The advantage of this approach is that the extinction coefficients computed from retrieved size distribution are less sensitive to errors in median radii as opposed to geometric standard deviations. The algorithm retrieves vertical profiles of liquid water content, number concentration, and effective radius using vertical profiles of radar reflectivity factor, Doppler velocity, and estimated particle median radius, together with integrated liquid water path. The median radius at each height within the cloud is estimated from a statistical model that relates variance of the vertical velocities in stratus to the stratus particle median radius. The input to the statistical model is the variance of the mean Doppler velocity (i.e., the first moment of the Doppler spectrum) measured by a 35-GHz Doppler radar computed for a given time period. Since the algorithm does not use shortwave radiation measurements, the results it produces are independent of any accompanying shortwave radiation measurements.

2. Method

a. Retrieval of number concentration and liquid water content

1) The lognormal distribution

We assume a lognormal number distribution for stratus cloud particles. A useful property of a lognormal distribution is that the nth moment can be calculated (Hinds 1982) as

$$\int_0^\infty f(r)r^n\,dr = r_n^n \exp\left(\frac{n^2 \ln^2\sigma_g}{2}\right), \tag{1}$$

where $f(r)$ is the lognormal cloud particle number distribution defined as

$$f(r) = \frac{N}{(2\pi)^{1/2} r \ln\sigma_g} \exp\left[\frac{-(\ln r - \ln r_n)^2}{2(\ln\sigma_g)^2}\right], \tag{2}$$

r is the particle radius, N is the particle number concentration, σ_g is the geometric standard deviation of the distribution, and r_n is the median radius. The median radius is defined as the radius for which half the particles are both smaller and larger than it.

2) Frisch et al. (1995, 1998) algorithm

Since radar reflectivity factor and liquid water content are proportional to the sixth and third moment of the cloud particle size distribution (White et al. 1991; Frisch et al. 1995), respectively, the reflectivity factor Z_i for the ith sample volume is

$$Z_i = 2^6 N_i r_{ni}^6 \exp(18 \ln^2\sigma_{gi}), \tag{3}$$

and the liquid water content, q_i, for the ith radar sample volume is

$$q_i = \frac{4}{3}\pi\rho_w N_i r_{ni}^3 \exp\left(\frac{9 \ln^2\sigma_{gi}}{2}\right), \tag{4}$$

where ρ_w is the density of liquid water. We can eliminate r_{ni} by combining (3) and (4) to obtain

$$q_i = \frac{1}{6}\pi\rho_w N_i^{1/2} \exp\left(-\frac{9}{2} \ln^2\sigma_{gi}\right) Z_i^{1/2}. \tag{5}$$

Summing the liquid water contents q_i over all radar sample volumes with height Δz_i yields the liquid water path,

$$Q = \frac{1}{6}\pi\rho_w N^{1/2} \exp\left(-\frac{9}{2} \ln^2\sigma_g\right) \sum_{i=1}^{n_c} Z_i^{1/2}\Delta z_i, \tag{6}$$

where n_c represents the number of in-cloud radar sample volumes. To obtain (6), we assume that $N_i^{1/2} \exp(-9/2 \ln^2\sigma_{gi})$ is constant with height (Ovtchinnikov and Kogan 2000). When we assume that N_i is constant with height and given all in-cloud radar reflectivity factors Z_i, the cloud liquid water path Q, and the geometric standard deviation σ_g, one can solve (6) for N (White et al. 1991; Frisch et al. 1995, 1998). Then N can subsequently be eliminated from (5) using (6) to obtain

$$q_i = Q\frac{Z_i^{1/2}}{\sum_{j=1}^{n_c} Z_j^{1/2}\Delta z_j}. \tag{7}$$

3) Proposed algorithm based on particle median radius estimation

Eliminating σ_{gi} from (3) and (4), as opposed to r_{ni}, we obtain

$$q_i = \frac{\sqrt{2}}{3}\pi\rho_w N_i^{3/4} r_{ni}^{3/2} Z_i^{1/4}. \quad (8)$$

When the liquid water contents q_i are summed over all radar sample volumes with height Δz_i, the liquid water path Q becomes

$$Q = \frac{\sqrt{2}}{3}\pi\rho_w N^{3/4} \sum_{i=1}^{n_c} r_{ni}^{3/2} Z_i^{1/4} \Delta z_i, \quad (9)$$

where the number concentration N is assumed to be constant with height. The particle median radius r_{ni} in (9) is estimated from the variance of the Doppler vertical velocity for each radar sample volume and hence varies with height. Eliminating N using (8) and (9), we obtain

$$q_i = Q \frac{r_{ni}^{3/2} Z_i^{1/4}}{\sum_{j=1}^{n_c} r_{nj}^{3/2} Z_j^{1/4} \Delta z_j}. \quad (10)$$

b. Determination of the particle median radius

Considine and Curry (1996) relate the vertical velocity distribution of parcels either ascending or descending adiabatically to the particle size distribution by assuming that the vertical velocity uniquely determines the particle size. They also assume that at a fixed height within a cloud and over a sufficiently long period of time the distribution of the vertical velocity is Gaussian and the mean velocity is zero. Consequently, parcels that reach a certain height can have different water contents, depending on their vertical velocities. A parcel that has a larger vertical velocity at a given height must have traveled a longer distance from its place of origin within cloud as compared to a parcel having a smaller vertical velocity at the same height. Since they assume that the vertical velocity of a parcel is zero at the lifting condensation level of the parcel, a diluted parcel that has lifted adiabatically within cloud has smaller vertical velocity than a nondiluted parcel originating from their respective lifting condensation levels.

As the variance of the vertical velocity increases, more parcels have higher saturation ratios, which leads to an increase in particle radii. In the Considine and Curry (1996) model the median radius r_{ni} and the variance of the vertical velocity are related as (see the appendix)

$$r_{ni} = \left(\frac{0.96\sqrt{2}}{D_i}\right)^{1/2}, \quad (11)$$

where

$$D_i = \frac{F_K + F_D}{\overline{ww}_i^{1/2}}\left(\frac{gX}{KT}\right) \quad \text{and} \quad (12)$$

$$X = \frac{\Gamma_e - \Gamma_p}{\Gamma_p - \Gamma_m}. \quad (13)$$

In these equations $\overline{ww}$ is the variance of the vertical velocity, g is the acceleration due to gravity, and T is the air temperature in the parcel. The symbols Γ_e, Γ_p, and Γ_m represent the environment, parcel, and moist adiabatic lapse rates, respectively; F_D, F_K, and K are defined in the appendix. Following Considine and Curry (1996), we assumed that X equals 2.4 and neglected the radius of the particles in a parcel of zero vertical velocity. When we use 850 hPa for p, 273 K for T, and 1.47×10^{10} s m^{-2} for $F_K + F_D$ (Rogers and Yau 1989, p. 104);

$$r_{ni} = 13.2\ \overline{ww}_i^{1/4}, \quad (14)$$

where r_{ni} is in micrometers and $\overline{ww}$ is in m^2 s^{-2}. In this study, we used (14) to retrieve r_{ni}.

According to Stokes' law, the fall velocity of a 10-μm radius spherical particle relative to air is approximately 1 cm s^{-1}. The variation in vertical air velocities of ± 1 m s^{-1} in one stratus cloud event observed by Sassen et al. (1999) indicates that the fall velocity of cloud particles relative to air is negligible. These results suggest that apart from drizzle particles the vertical velocities of cloud particles are close to the velocity of air. Because the formation of stratus clouds is over scales of motion that encompass a radar sample volume and the statistical model of Considine and Curry (1996) is based on the distribution of vertical velocities that drives the vertical motion of parcels, and not individual cloud particles, we assume that the first moment of the Doppler radar spectrum, or the mean Doppler velocity v_d represents w in the Considine and Curry (1996) study. We further assume that the mean Doppler velocity v_d averaged over a 30-min interval is approximately zero, so that $\overline{v_d v_d}$ is a reasonable measure of $\overline{ww}$. To eliminate possible biases in v_d as a measure of the vertical air motion that result from precipitating particles we limited the analysis to radar data with Doppler velocities between ± 1 m s^{-1} and with reflectivity factors less than -20 dBZ.

The mean Doppler velocity v_d averaged over the 30-min interval may depart from zero, and hence $\overline{v_d v_d}$ may not be a perfect estimator for $\overline{ww}$. In addition, $\overline{v_d v_d}$ depends on the sampling frequency of the Doppler velocity measurements. The magnitude of the error in $\overline{v_d v_d}$ and how well $\overline{v_d v_d}$ represents $\overline{ww}$ are difficult to quantify; however, the sensitivity of the median radius to the error in the variance is not large (see section 4).

c. Retrieval of effective radius

Hu and Stamnes (1993) demonstrated that an important parameter for quantifying the impact of clouds on the radiation field is the effective radius r_e which is defined by Hansen and Travis (1974) as

$$r_e = \frac{\int_0^\infty f(r) r^3 \, dr}{\int_0^\infty f(r) r^2 \, dr}. \quad (15)$$

Therefore, we must relate N, q_i, and r_{ni} to r_{ei} to use the retrieved results in radiative transfer studies. Again assuming a lognormal number distribution for $f(r)$, the effective radius r_{ei} is

$$r_{ei} = r_{ni} \exp(2.5 \ln^2 \sigma_{gi}). \quad (16)$$

Using the relation

$$\exp(\ln^2 \sigma_{gi}) = r_{ni}^{-(2/9)} \left(\frac{\pi \rho_w Z_i}{48 q_i} \right)^{2/27}, \quad (17)$$

which is derived from (3) and (4), to eliminate σ_{gi} in (16), we obtain

$$r_{ei} = r_{ni}^{4/9} \left(\frac{\pi \rho_w Z_i}{48 q_i} \right)^{5/27}. \quad (18)$$

3. Results

We used data collected at the Atmospheric Radiation Measurement (ARM) program (Stokes and Schwartz 1994) Southern Great Plains central facility (36.69°N, 97.48°W) to retrieve the size distribution of stratus cloud particles. We retrieved vertical profiles of cloud liquid water content, number concentration, and effective radius during two stratus cloud cases that occurred over the central facility. The first case was 30 April 1994 when a single layer stratus cloud passed over the site in the afternoon (Sassen et al. 1999). While the retrieval developed by Liljegren (1995) provided estimates of cloud liquid water path from microwave radiometer measurements, the University of Massachusetts 35-GHz Doppler radar provided radar reflectivity factor and Doppler velocity observations from 2030 to 2200 UTC. During the entire period, the reflectivity factors measured by the radar were less than −20 dBZ, suggesting the absence of drizzle. The general lack of drizzle during this period is also supported by surface observations that recorded no precipitation. Note that for approximately 6 min around 2130 UTC the cloud radar reflectivity factors were below the threshold of detection.

The second case took place on 3 December 1997 when a single layer stratus cloud covered the site. Reflectivity factors and Doppler velocities were measured by the ARM 35-GHz Doppler radar operated as a part of the Atmospheric Radiation Measurement program (Moran et al. 1998; Clothiaux et al. 2000). The clouds were thick and precipitating from 0000 to 0600 UTC. During this period, the radar detected hydrometers up to 8 km with a maximum reflectivity factor of approximately 10 dBZ. The clouds subsequently thinned and single layer stratus cloud covered the site from 1200 to 2400 UTC. During this period, radar reflectivity factors were less than −25 dBZ and no precipitation was recorded at the surface. The low radar reflectivity factors for these two cases also imply that these clouds were liquid water clouds (Mace and Sassen 2000).

The retrieved liquid water contents, particle effective radii, and number concentrations for the 30 April and 3 December cases are presented in Figs. 1 and 2, respectively. As Figs. 1 and 2 illustrate, cloud liquid water contents were higher on 30 April compared to 3 December, and in both cases the maximum liquid water content ($\approx$1.0 g m^{-3} at 2100 UTC on 30 April and $\approx$0.4 g m^{-3} at 2100 UTC on 3 December) occurred when cloud top reached its maximum altitude. However, the same amount of liquid water content occurred near 1400 UTC when the cloud altitude is minimum on 3 December 1997. In the two cases the retrieved liquid water contents increased with height through the lower half or two-thirds of the stratus (Fig. 3), in agreement with both theoretical studies (Mason and Chien 1962; Khairoutdinov and Kogan 1999) and observations (Albrecht et al. 1985, 1990; Noonkester 1984; Stephens and Platt 1987). Averaging the liquid water content profiles from 2111 to 2142 UTC (apart from the break in cloud around 2130 UTC) on 30 April led to a maximum of 0.63 g m^{-3} at an altitude of 1.6 km above ground level, in agreement with the results of Sassen et al. (1999).

Sassen et al. (1999) report that in situ observations in the stratus with a forward scattering spectrometer probe (FSSP) from 2111 to 2142 UTC on 30 April led to an average value of 345 cm^{-3} for the number concentration that was fairly constant with height. The retrieved number concentration averaged over the same period was 338 cm^{-3}.

Since we assume a constant number concentration with height and the retrieved cloud liquid water increases with height, the retrieved particle effective radius increased with height (Fig. 3). This increase in the particle effective radius with height also agrees with observations (Nicholls 1984; Stephens and Platt 1987). The average volume radii, r_{vi}, which is the radius of a particle the mass of which equals the liquid water content divided by the number concentration, derived from the retrieval and in situ FSSP measurements made on 30 April increase with height and are comparable in magnitude (Fig. 4).

To further evaluate the reasonableness of the retrieved microphysical properties, we input them into two radiative transfer models and compared the results with observations. To this end we used delta two- and four-stream radiative transfer models (Toon et al. 1989; Liou et al. 1988) to compute the downward longwave and shortwave surface irradiance, respectively, using the retrieved number concentrations and effective radii as input to these models. We computed the optical properties of the cloud particles according to Mie theory using the retrieved effective radius and a geometric standard de-

viation of 1.42 to specify the parameters of a lognormal distribution.

In the radiative transfer calculations gaseous absorption was computed using the *k*-distribution tables with the correlated-*k* assumption developed by Kato et al. (1999) and Mlawer et al. (1997) for shortwave and longwave radiation, respectively. Rawinsondes provided atmospheric water vapor profiles for both case study periods, while we estimated the shortwave surface albedo for 3 December from the ratios of upward to downward pointing pyranometer measurements. The average surface albedo between 1800 and 2100 UTC on 3 December was 0.174, and we used this value for the surface albedo on 30 April because the upward surface irradiance was not measured on this day. We assumed the surface emissivity to be unity and used the surface air temperature for the surface temperature. Both the downward shortwave and downward longwave irradiances were computed at 1-min intervals over the two case study periods.

The resulting downward shortwave surface irradiances are well correlated with the measured irradiances between 2030 and 2200 UTC on 30 April (Fig. 5) and throughout the 8-h period from 1400 to 2200 UTC on 3 December (Fig. 6). On average, the modeled shortwave irradiance is greater by 21 W m^{-2} and smaller by 6.3 W m^{-2} than the measurements on 30 April and 3 December, respectively. These amounts correspond to 12% and 8% of the averaged measured downward shortwave irradiance for these two periods. The modeled longwave irradiance is smaller by 0.7 W m^{-2} than the measurements for the both days, which corresponds to 0.2% of the averaged measured downward longwave irradiance over the two periods.

In order to check the consistency for the 3 December 1997 case, we computed extinction coefficients by

$$\beta_i = \frac{3q_i}{2\rho_w r_{ei}}, \tag{19}$$

and integrated over the cloud height to compare with optical thicknesses used for the computation of irradiances (Fig. 7). The optical thickness integrated from (19) is approximately 1.6 times larger than those used in the computation. To estimate the significance of these optical thickness differences, we compute the irradiance by multiplying the number concentration by 1.6 so that the extinction coefficients are close to those computed by (19). While it is possible that the difference is caused by inhomogeneity of clouds because the radar only provide cloud information at the zenith and the model uses plane-parallel clouds, approximations in the algorithm and instrumental errors can cause the difference. Possible reasons of these optical thickness differences are addressed in the next section along with sensitivity studies.

For the comparison, we also used the effective radius of 5.4 μm, which is the average effective radius for continental stratus clouds reported by Miles et al. (2000), to compute the downward shortwave and longwave surface irradiance. The liquid water was uniformly distributed from the observed cloud base to the top. The computed irradiance with the average effective radius is also well correlated with measurements, which implies that the variation of the shortwave surface irradiance is mainly caused by the variation in the liquid water path. On average, the modeled shortwave irradiance with the average effective radius is greater by 13 W m^{-2} and smaller by 23 W m^{-2} than the measurements on 30 April and 3 December, respectively. While Dong et al. (2000) reported a substantial variation in the effective radius over 2 yr at the site (4–14 μm), using the effective radius of 5.4 μm for computing downward irradiance does not introduce a significant bias error for these two cases because the retrieved effective radii are close to the average effective radius.

4. Discussion

When a cloud extends through n_c radar sample volumes, there are $n_c + 1$ equations in the retrieval consisting of n_c equations of (3) and one equation of (9). Assuming a lognormal distribution for each radar sample volume produces a total of $3n_c$ unknowns, that is, N_i, σ_{gi}, and r_{ni} for each radar sample volume. Therefore, we must make assumptions to reduce the number of unknowns from $3n_c$ to $n_c + 1$. Following White et al. (1991), we made the assumption that the number concentration N_i was constant with height. We then used the variance of the vertical Doppler velocity to obtain r_{ni} throughout the vertical extent of cloud and solved the resulting $n_c + 1$ equations for N and σ_{gi} ($i = 1, \ldots, n_c$).

Since the liquid water content q_i, effective radius r_{ei}, number concentration N, and extinction coefficient β_i, are important to the radiation, we must quantify how errors in the estimates of the retrieved properties, and especially r_{ni}, propagate into estimates of these radiatively important quantities. In the following section, we estimated the error in retrieved values due to the error in the estimated median radius. For a comparison, we also estimated the error in retrieved values by the algorithm given by Frisch et al. (1995) due to the error in the geometric standard deviation. To estimate the error in the liquid water content due to the error in the median radius, we use (10) and take the derivative with respect to r_{ni} to obtain

$$\frac{\partial q_i}{\partial r_{ni}} = \frac{3}{2}\left(\frac{q_i}{r_{ni}} - \frac{q_i r_{ni}^{1/2} Z_i^{1/4} \Delta z_i}{\sum_{j=1}^{n_c} r_{nj}^{3/2} Z_j^{1/4} \Delta z_i}\right). \tag{20}$$

When we sum the error contributing to the ith radar sample volume from other radar sample volumes (i.e., $(\partial q_i/\partial r_{nk})\Delta r_{nk}$, $k \neq i$), the error in the liquid water content is

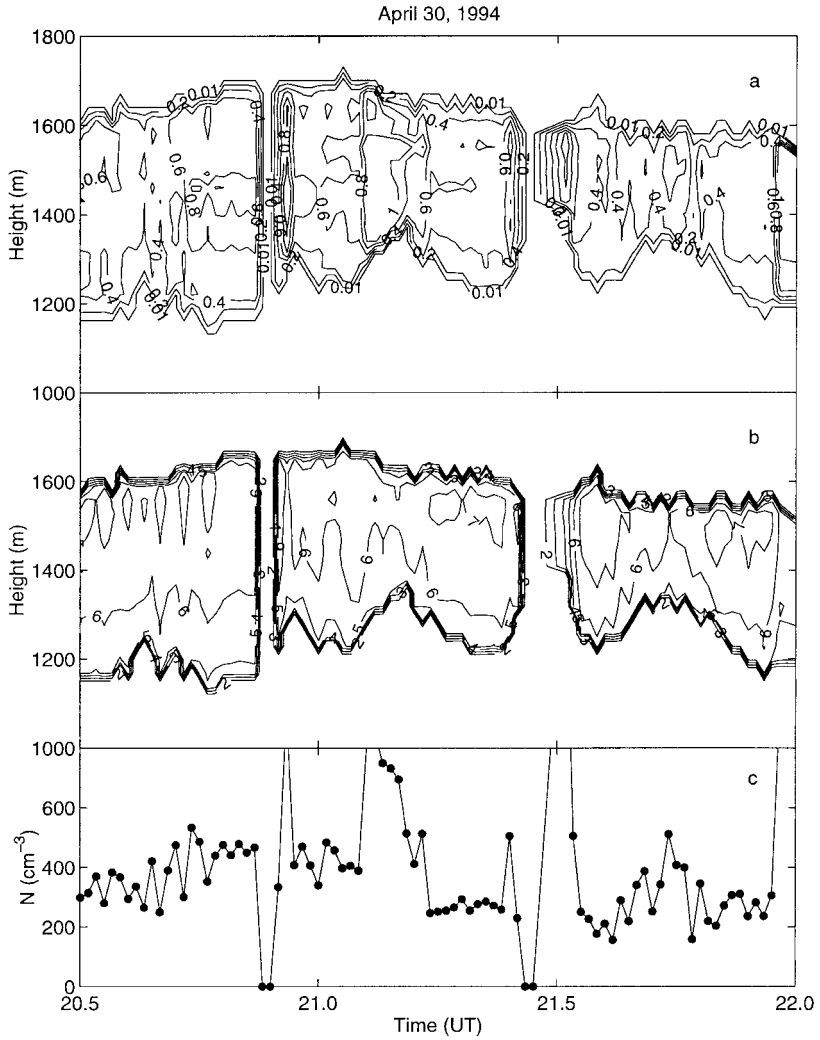

FIG. 1. Retrieved (a) liquid water contents, (b) effective radii, and (c) number concentrations for 30 Apr 1994. The radar reflectivity factor is averaged every minute to produce the contour plot. The contour interval in (a) is every 0.2 g m^{-3} and numbers indicate the liquid water content (in g m^{-3}). The contour interval in (b) is every micrometer and numbers indicate the radius (in μm).

$$\frac{\Delta q_i}{q_i} = \frac{3}{2}\left(\frac{\Delta r_{\mathrm{ni}}}{r_{\mathrm{ni}}} - \frac{\sum_{j=1}^{n_c} r_{\mathrm{nk}}^{1/2} Z_k^{1/4} \Delta z_k \Delta r_{\mathrm{nk}}}{\sum_{j=1}^{n_c} r_{\mathrm{nj}}^{3/2} Z_j^{1/4} \Delta z_j}\right). \tag{21}$$

When the fractional error in the median radius does not depend on height, the error in the liquid water content vanishes. The liquid water content retrieved by the algorithm given by Frisch et al. (1995) does not depend on the value of geometric standard deviation because of the assumption of the constant geometric standard deviation with height.

To further investigate the error in the effective radius, we define the average volume radius, r_{v}, the radius of a particle of which mass times the number concentration gives the liquid water content, as

$$r_{\mathrm{vi}} = \left(\frac{3q_i}{4\pi\rho_{\mathrm{w}} N}\right)^{1/3}. \tag{22}$$

For a lognormal distribution, the effective radius, r_{ei}, is

$$r_{\mathrm{ei}} = r_{\mathrm{vi}} \exp(\ln^2 \sigma_{\mathrm{gi}}). \tag{23}$$

Combining (17), (22), and (23) yields

$$r_{\mathrm{ei}} = r_{\mathrm{ni}}^{-(2/9)} \left(\frac{3q_i}{4\pi\rho_{\mathrm{w}} N}\right)^{1/3} \left(\frac{\pi\rho_{\mathrm{w}} Z_i}{48 q_i}\right)^{2/27}. \tag{24}$$

Substituting (9) for N and (10) for q_i in (24) and taking the derivative with respect to r_{ni} yields

$$\frac{\partial r_{\mathrm{ei}}}{\partial r_{\mathrm{ni}}} = \frac{r_{\mathrm{ei}}}{r_{\mathrm{ni}}}\left(\frac{1}{6} + \frac{5 r_{\mathrm{ni}}^{3/2} Z_i^{1/4} \Delta z_i}{18 \sum_{j=1}^{n_c} r_{\mathrm{nj}}^{3/2} Z_j^{1/4} \Delta z_j}\right). \tag{25}$$

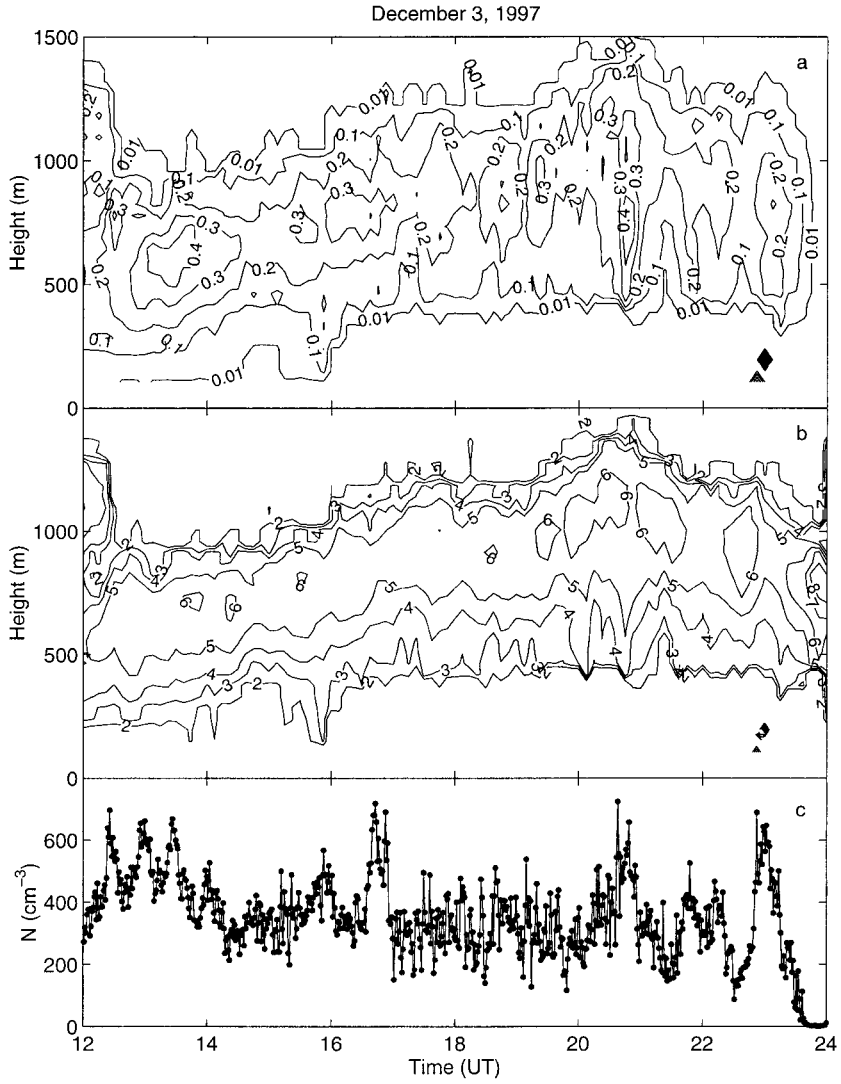

FIG. 2. Retrieved (a) liquid water contents, (b) effective radii, and (c) number concentrations for 3 Dec 1997. The radar reflectivity factor is averaged every 7.5 min to produce the contour plot. The contour interval in (a) is every 0.1 g m^{-3} and numbers indicate the liquid water content (in g m^{-3}). The contour interval in (b) is every micrometer and numbers indicate the radius (in μm).

Again, when we sum the error contributing to the *i*th radar sample volume from other radar sample volumes, the error in the effective radius is

$$\frac{\Delta r_{ei}}{r_{ei}} = \frac{\Delta r_{ni}}{6r_{ni}} + \frac{5\sum_{k=1}^{n_c} r_{nk}^{1/2} Z_k^{1/4} \Delta z_k \Delta r_{nk}}{18\sum_{j=1}^{n_c} r_{nj}^{3/2} Z_j^{1/4} \Delta z_j}. \quad (26)$$

When the fractional error in the median radius does not depend on height, (26) becomes

$$\frac{\Delta r_{ei}}{r_{ei}} = \frac{4\Delta r_{ni}}{9r_{ni}}. \quad (27)$$

Therefore, the fractional error in the r_{ei} is approximately half of the fractional error in r_{ni} when the fractional error in the median radius does not depend on height, hence the shape of the median radius vertical profile is correct. Similarly, substituting (6) for N in (22), substituting the resulting equation in (23), and taking the derivative with respect to σ_g, we obtain

$$\frac{\partial r_{ei}}{\partial \sigma_g} = -\frac{4r_{ei} \ln \sigma_g}{\sigma_g}. \quad (28)$$

Hence, the fractional error in the effective radius retrieved by the algorithm given by Frisch et al. (1995) is 1.3 times greater than the fractional error in the geometric standard deviation when the geometric standard deviation is 1.4.

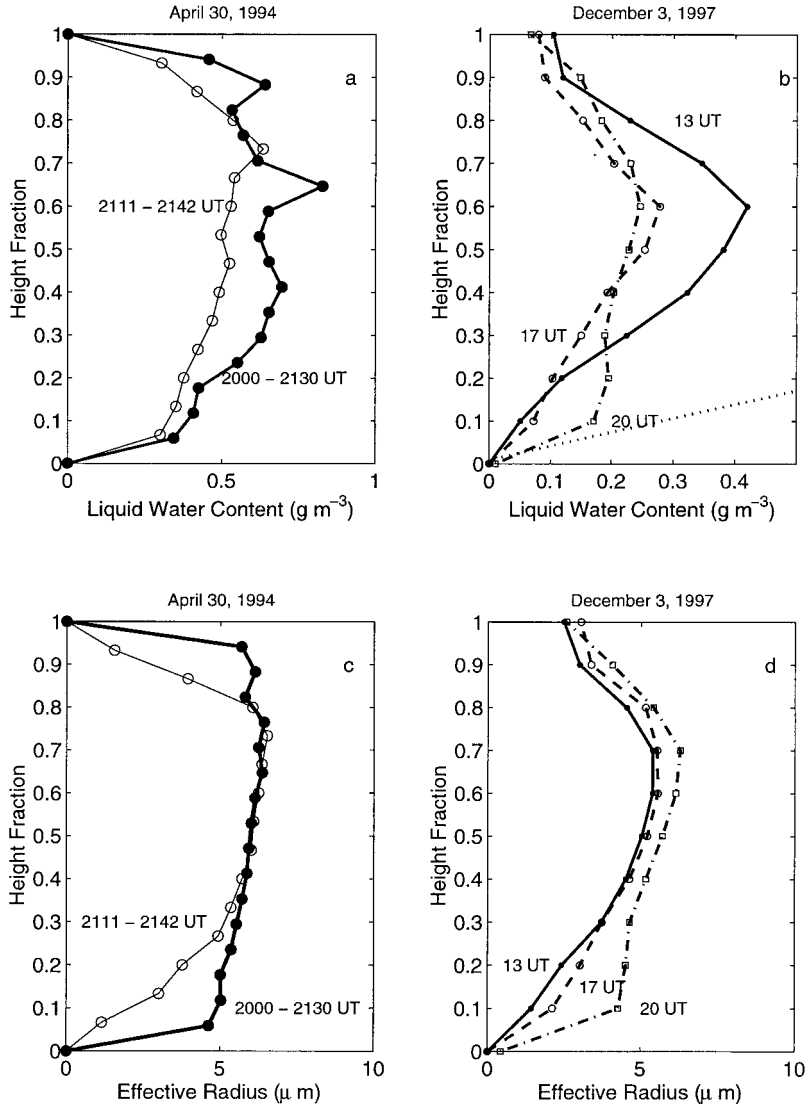

FIG. 3. Vertical profile of the liquid water content and effective radius for 30 Apr 1994 [(a) and (c), respectively] and 3 Dec 1997 [(b) and (d), respectively]. The ordinate is the fraction of the height relative to the cloud depth. The dotted line in (b) indicates the adiabatic liquid water content.

To estimate the sensitivity of the number concentration to errors in the estimate of value r_{ni}, we take the derivative of N with respect to r_{ni} in (9) and add the error due to all in-cloud radar sample volumes, the error in the number concentration is

$$\frac{\Delta N}{N} = -2\frac{\sum_{k=1}^{n_c} r_{nk}^{1/2} Z_k^{1/4} \Delta z_k \Delta r_{nk}}{\sum_{j=1}^{n_c} r_{nj}^{3/2} Z_j^{1/4} \Delta z_j}. \tag{29}$$

If the fractional error in the median radius does not depend on height, (29) becomes

$$\frac{\Delta N}{N} = -2\frac{\Delta r_{ni}}{r_{ni}}. \tag{30}$$

That is, the fractional error in the number concentration is approximately twice as large as the fractional error in r_n and opposite in sign. For comparison to the retrievals based on a constant value of σ_g we take the derivative of N with respect to σ_g in (6) to obtain

$$\frac{\partial N}{\partial \sigma_g} = \frac{18N \ln \sigma_g}{\sigma_g}. \tag{31}$$

Since the value of 18 In σ_g is approximately 6 when σ_g is 1.4, the fractional error in N is six times larger than the fractional error in σ_g.

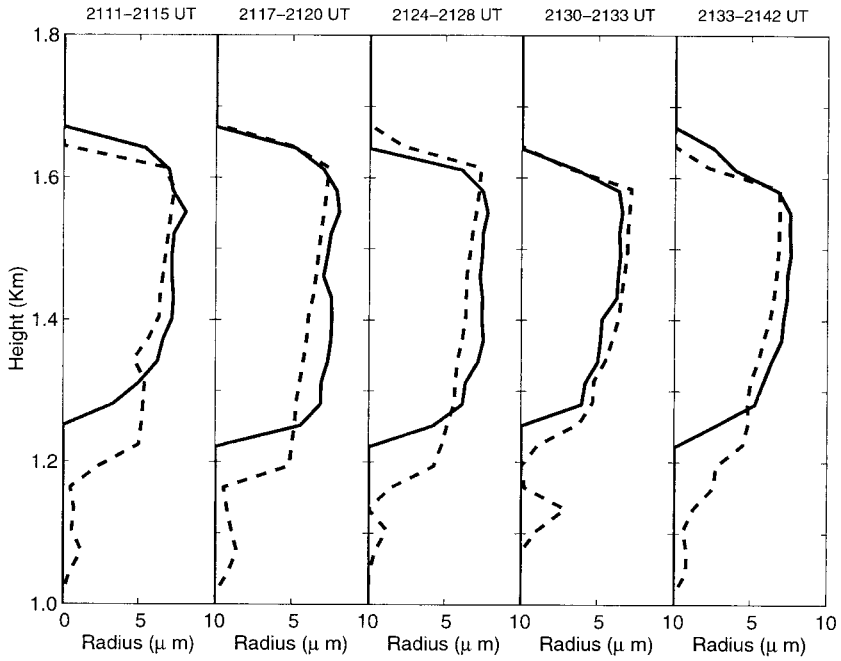

FIG. 4. Profiles of the average volume radius, which is the radius of particle of which mass equals the liquid water content divided by the number concentration, derived from the airborne laser-based FSSP data (dashed line) and from retrieved size distributions (solid line). The volume mean radii are averaged over time periods indicated at the top of the figure.

If we assume that the shortwave extinction coefficient β_i is given by (19), then

$$\frac{1}{\beta_i}\frac{\partial \beta_i}{\partial r_{\rm ni}} = \frac{1}{q_i}\frac{\partial q_i}{\partial r_{\rm ni}} - \frac{1}{r_{\rm ei}}\frac{\partial r_{\rm ei}}{\partial r_{\rm ni}}. \tag{32}$$

Substituting (20) and (25) into (32) and summing the error due to all in-cloud radar sample volumes yields

$$\frac{\Delta\beta_i}{\beta_i} = \frac{4\Delta r_{\rm ni}}{3r_{\rm ni}} - \frac{16\sum_{k=1}^{n_c} r_{\rm nk}^{1/2} Z_k^{1/4}\Delta z_k \Delta r_{\rm nk}}{9\sum_{j=1}^{n_c} r_{\rm nj}^{3/2} Z_j^{1/4}\Delta z_j}. \tag{33}$$

When we add the error due to all in-cloud radar sample volumes and if the fractional error in the median radius is independent with height, (33) becomes

$$\frac{\Delta\beta_i}{\beta_i} = -\frac{4\Delta r_{\rm ni}}{9r_{\rm ni}}. \tag{34}$$

Likewise, the fractional error in the extinction coefficient as a result of error in the geometric standard deviation in the algorithm given by Frisch et al. (1995) is

$$\frac{\Delta\beta_i}{\beta_i} = 4\ln\sigma_{\rm g}\frac{\Delta\sigma_{\rm g}}{\sigma_{\rm g}}. \tag{35}$$

The fractional error in β_i is approximately half of the fractional error in $r_{\rm ni}$ if the fractional error in the median radius does not depend on height and about 1.3 times the fractional error in $\sigma_{\rm g}$ when $\sigma_{\rm g}$ is 1.4. Note that the error in q_i vanishes when the fractional error in $r_{\rm ni}$ is independent with height so that the magnitude of error in β_i is the same as the magnitude of error in $r_{\rm ei}$.

In a study of in situ cloud measurements Miles et al. (2000) report that the median radius observed in stratus clouds varies from 1 to 10 μm, while the geometric standard deviation varies from 1.2 to 2.2. Therefore, the variations in the median radius and geometric standard deviation are significant, implying that neither quantity should be set to a climatological average for the most accurate retrievals. However, using the effective radius of 5.4 μm, which is the average effective radius of continental stratus clouds, for computing downward irradiance does not introduce a significant bias error because the retrieved effective radii for these two cases are close to the average effective radius. If the effective radius of stratus at given site does not change very much and if the value is known, using the value for the surface irradiance may give the unbiased irradiance when they are averaged over a certain period. However, Dong et al. (2000) reported a substantial variation in the effective radius at the site.

In this study we used the variance of the vertical Doppler velocity to estimate the median radius $r_{\rm ni}$, which is a function of $D_{\rm i}$ given by (12). The sensitivity of $r_{\rm ei}$ to D_i is given by

$$\frac{\partial r_{\rm ei}}{\partial D_i} = \frac{\partial r_{\rm ei}}{\partial r_{\rm ni}}\frac{\partial r_{\rm ni}}{\partial D_i}. \tag{36}$$

The sensitivity of $r_{\rm ni}$ to D_i is

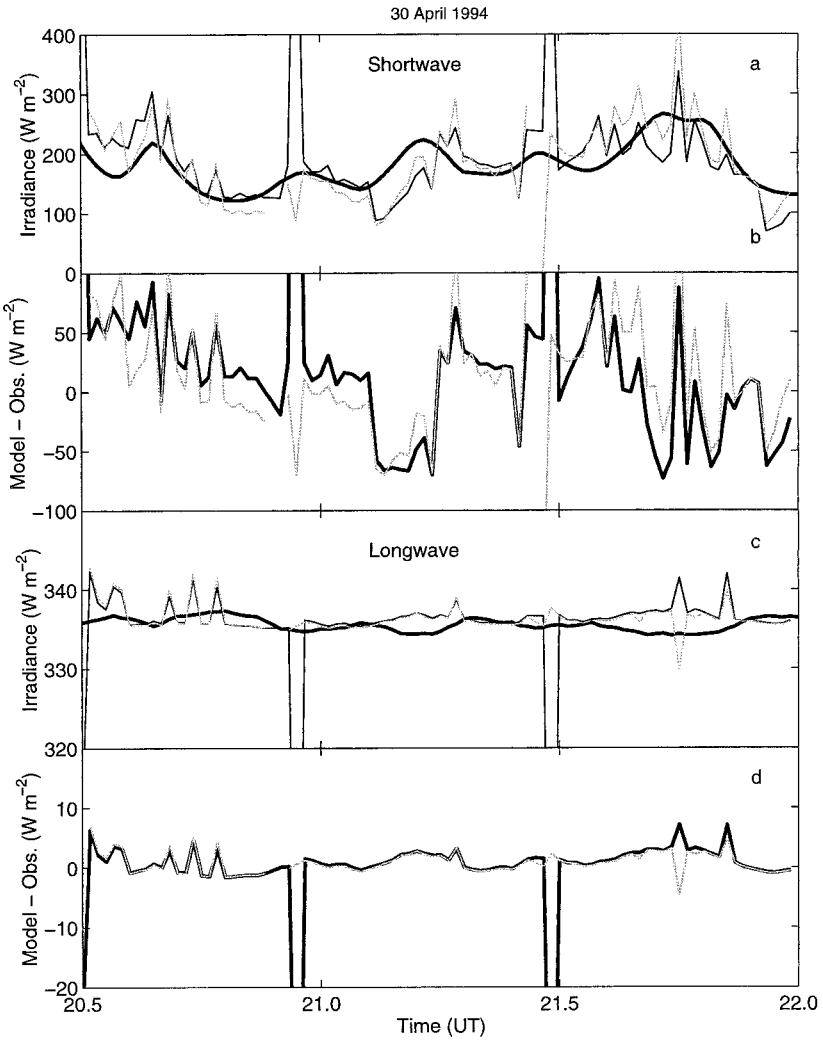

FIG. 5. Measured (thick line) (a) shortwave and (c) longwave downward irradiance at the surface on 30 Apr 1994. The thin and shaded solid lines indicate the modeled irradiance with retrieved size distributions and with 5.4-μm effective radius, respectively. The retrieved effective radius and concentration were used to compute the irradiance for every minute. Shortwave case (b) and longwave case (d) show the difference of the modeled irradiance with retrieved size distribution (thick solid line) and with 5.4 μm (shaded line) from the measurements.

$$\frac{\partial r_{\mathrm{ni}}}{\partial D_i} = -\frac{r_{\mathrm{ni}}}{2D_i}, \tag{37}$$

where $r_{\mathrm{n}}^2 D = 0.96\sqrt{2}$ when $r_0 = 0$ is used to derive (37). Consequently, the fractional error in r_{ni} is half of the fractional error in D_i and the fractional error in r_{ei} due to the error in D_i is approximately one-fourth of the fractional error in D_i if the fractional error in r_{ni} does not depend on height. Considine and Curry (1996) show that D is not a strong function of temperature but changes with $\overline{ww}$ and X. While $\overline{ww}$ was estimated from measurements, X was assumed to be 2.4 in the retrieval. The quantity X can vary from zero to infinity depending on the lapse rate of the parcel relative to the environmental and adiabatic lapse rates. For realistic values of r_{ni}, X must be between 1 and 4 if the maximum of $\overline{ww}$ is approximately 0.2 m^2 s^{-2}, which was the case for the two study periods.

To verify the magnitude of the preceding error estimates we constructed a simple five-layer cloud model with layer median radii and geometric standard deviations given in Table 1. We then retrieved the effective radius, number concentration, and liquid water content for each layer with either the median radii or geometric standard deviations set to their perturbed values in Table 1. The case indicated by "r_{ni} perturbation" in Table 1 simulates the retrieval proposed in this paper and that by "σ_{g} set to 1.4" simulates the retrieval given by Frisch et al. (1995). We subsequently computed the extinction coefficients β_i using (19).

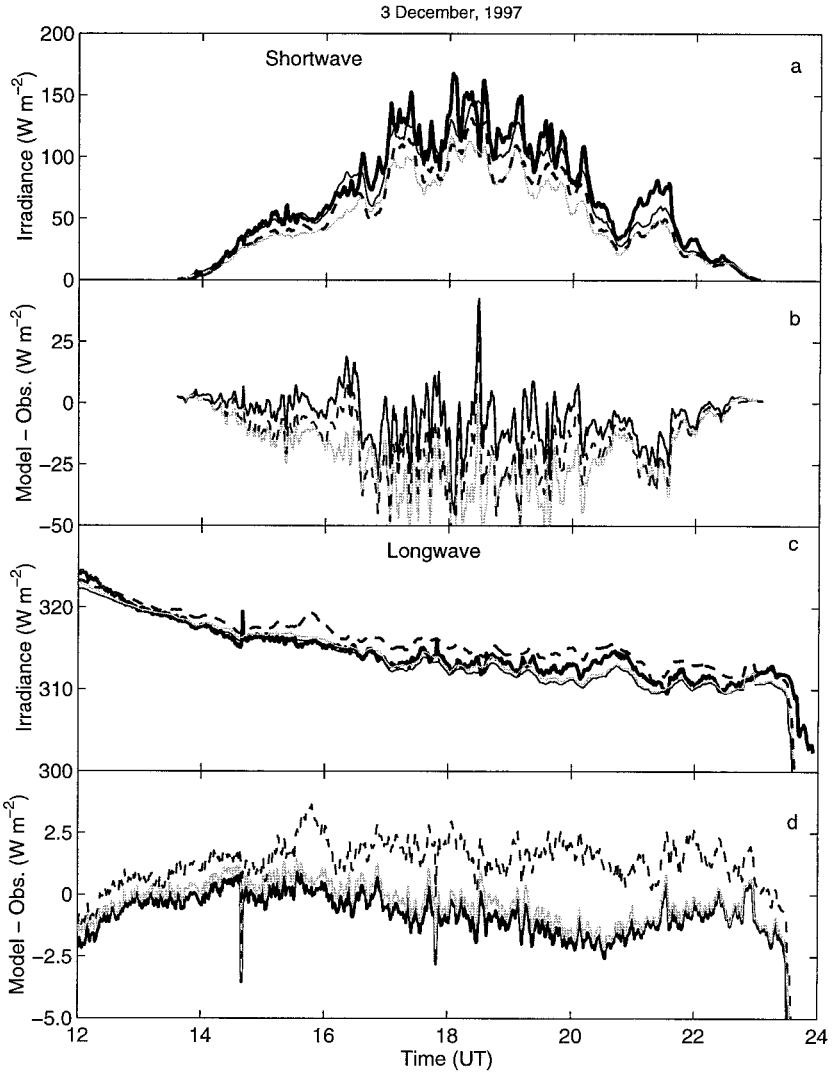

FIG. 6. Measured (thick line) (a) shortwave and (c) longwave downward irradiance at the surface on 3 Dec 1997. The thin and shaded solid lines indicate the modeled irradiance with retrieved size distributions and with 5.4-μm effective radius, respectively. Inputs to compute irradiances indicated by the dashed line are the same as the thin line except that the number concentration is multiplied by 1.6. The retrieved effective radius and concentration were used to compute the irradiance for every minute. Shortwave case and longwave case (d) show the difference of the modeled irradiance with retrieved size distribution (thick solid line) and with 5.4 μm (shaded line) from the measurements for 3 Dec 1997.

The results from this simple model are in agreement with the preceding error analysis. For example, when r_n is perturbed to a value approximately 20% smaller than the actual r_n, r_{ei} given by (16) decreases by approximately 10% and N given by (9) increases by approximately 80%. The resulting extinction coefficient increases by approximately 10%. Similarly, when σ_g is set to a value of 1.4 (a perturbation to a value approximately 20% greater than the actual σ_g), r_e decreases by approximately 15% and N given by (6) increases by approximately 120%. In this case the extinction coefficient increases by approximately 15%. All of these changes are what is expected based on (20)–(35).

In many cases the particle size distributions in stratus clouds may not be a single-mode lognormal distribution (e.g., Nicholls 1984). In order to estimate the error introduced into the retrieval by assuming a single lognormal size distribution for cloud particles, we applied the retrieval to a bimodal distribution of cloud particles (Table 1, case 2). To generate a bimodal distribution we added particles with a median radius of 30 μm, a geometric standard deviation of 1.4, and a concentration of 1.0 cm^{-3} to the case 1 value of r_{ni} and a geometric standard deviation of 1.4. We then retrieved N, r_{ei}, and q_i both assuming the size distribution of the smaller particles. In both cases the retrieved number concentra-

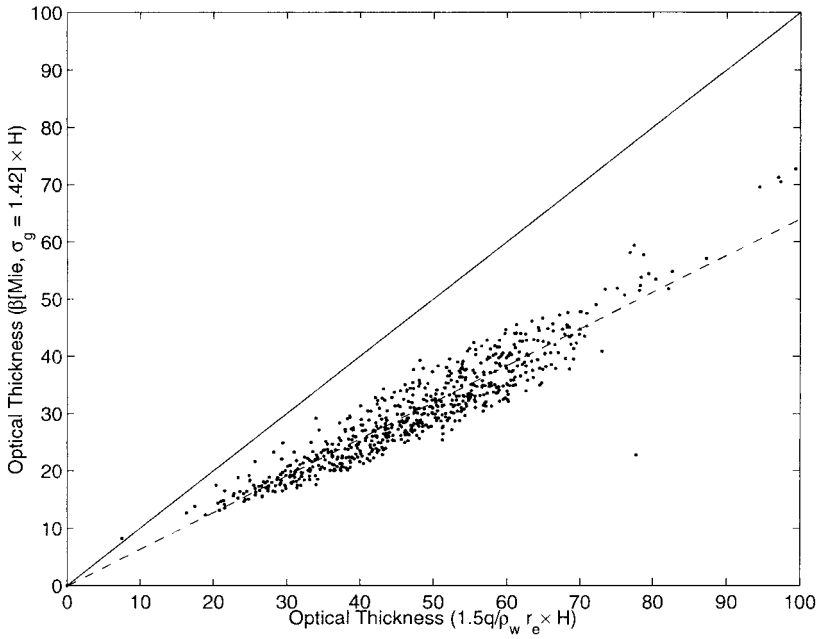

FIG. 7. Optical thicknesses computed by integrating extinction coefficients given by Mie theory vs those computed by integrating extinction coefficients given by (19). Retrieved effective radii with the fixed geometric standard deviation of 1.42 are used to compute the extinction cross sections by Mie theory, which are used for irradiance computations.

tions, N, is less than its actual value. However, the number concentration obtained by setting σ_g to 1.4 is much smaller. To understand this result rewrite (6) and (9) as

$$\left(\frac{Q}{\rho_w \sum_{i=1}^{n_c} Z_i^{1/2} \Delta z_i}\right)^2 = \frac{\pi^2}{36 \exp(9 \ln^2 \sigma_g)} N \quad \text{and} \quad (38)$$

$$\left(\frac{Q}{\rho_w \sum_{i=1}^{n_c} Z_i^{1/4} \Delta z_i}\right)^{4/3} = \left(\frac{\sqrt{2}}{3}\pi\right)^{4/3} r_n^2 N, \quad (39)$$

respectively. For simplicity assume that r_{ni} is constant with height. Both sides of (38) have dimensions of one over length cubed, while the both sides of (39) have dimensions of one over length. By adding large particles to a single-mode lognormal distribution (as in case 2), the left-side denominator in (38) is augmented more than in (39), causing a larger change in N.

We also investigated, in Table 2, sensitivities of retrieval values to instrumental errors to the true value given at the top of Table 2. Clothiaux et al. (1995) show that the one-way attenuation rate of 94-GHz radar signals is less than 5 dB km^{-1} when the liquid water content is less than 1 g m^{-3} and the mean radius is approximately 5 μm. Attenuation of 35-GHz radar signals is about one-sixth of 94-GHz radar signals, which gives attenuation no more than 1 dB km^{-1} in the same cloud. In this study, first, we assumed the two-way attenuation of radar signal of 0.5 dB in each layer (case 1 in Table 2). Second, we assumed that radar reflectivity factors of all layers are 3 dB smaller than the true values due to the calibration error (case 2 in Table 2). In both cases the reflectivity factor is smaller than the reflectivity factor computed from the liquid water content. In order to tolerate these reductions in reflectivity factor keeping the liquid water path the same as in the algorithm, the size of particles must be reduced and the number concentration must be increased because reflectivity factor is more sensitive to the particle size. For both cases the extinction coefficient computed from the retrieved size distribution were increased due to increasing the number concentration because increasing the left side of (38) and (39) by attenuation or the calibration error increases N in the right side. Third, we increased the liquid water path by 10% (case 3 in Table 2). In all three cases, the optical thicknesses of the cloud integrated from extinction coefficients are greater than the true values. However, the optical thicknesses computed from the proposed retrieval results are affected less by these instrumental errors than those computed from the Frisch et al. (1995) retrieval.

One drawback of the proposed retrieval based on estimates of the median radius r_{ni} is that the geometric standard deviation becomes imaginary (i.e., $\ln^2 \sigma_g < 0$) when the retrieved effective radius is less than r_{ni}. In other words, when our estimate of the median radius is larger than the retrieved effective radius because of assumptions in the algorithm or instrumental errors or both, the geometric standard deviation is unphysical. Even when the retrieved standard deviation is unphys-

TABLE 1. Sensitivity study of retrieval algorithm. Numbers in parentheses indicate the assumed values.

Layer	r_n (μm)	σ_g	Z (dBZ)	q (g m^{-3})	r_e (μm)	N (cm^{-3})	β (m^{-1})
Case 1 cloud, truth							
1	7.0	1.1	−24	0.60	7.2	400	0.13
2	8.0	1.1	−21	0.89	8.2	400	0.16
3	7.0	1.1	−24	0.60	7.2	400	0.13
4	6.0	1.2	−26	0.42	6.5	400	0.10
5	5.0	1.2	−31	0.24	5.4	400	0.07
Case 1 cloud, proposed retrieval, r_{ni} perturbation							
1	(5.1)	1.3	(−24)	0.57	6.3	737	0.13
2	(5.8)	1.3	(−21)	0.84	7.2	737	0.18
3	(5.1)	1.3	(−24)	0.57	6.3	737	0.13
4	(5.0)	1.3	(−26)	0.49	6.1	737	0.12
5	(4.2)	1.3	(−31)	0.29	5.1	737	0.08
Case 1 cloud, Frisch et al. (1995) retrieval, σ_g set to 1.4							
1	4.6	(1.4)	(−24)	0.58	6.1	877	0.14
2	5.3	(1.4)	(−21)	0.87	7.0	877	0.19
3	4.6	(1.4)	(−24)	0.58	6.1	877	0.14
4	4.1	(1.4)	(−26)	0.46	5.4	877	0.13
5	3.4	(1.4)	(−31)	0.26	4.5	877	0.09
Case 2 cloud, truth							
1	7.0 + 30.0	1.4 + 1.4	−4	1.14	9.3 + 39.8	400 + 1	0.16
2	8.0 + 30.0	1.4 + 1.4	−3	1.62	10.6 + 39.8	400 + 1	0.21
3	7.0 + 30.0	1.4 + 1.4	−4	1.14	9.3 + 39.8	400 + 1	0.16
4	6.0 + 30.0	1.4 + 1.4	−4	0.79	8.0 + 39.8	400 + 1	0.12
5	5.0 + 30.0	1.4 + 1.4	−4	0.54	6.6 + 39.8	400 + 1	0.09
Case 2 cloud, proposed retrieval, r_{ni} perturbation							
1	(7.0)	1.8	(−4)	1.13	15.4	206	0.11
2	(8.0)	1.7	(−3)	1.41	15.5	206	0.14
3	(7.0)	1.8	(−4)	1.13	15.4	206	0.11
4	(6.0)	1.8	(−4)	0.89	15.3	206	0.09
5	(5.0)	1.9	(−4)	0.67	15.1	206	0.07
Case 2 cloud, Frisch et al. (1995) retrieval, σ_g set to 1.4							
1	18.3	(1.4)	(−4)	1.05	24.4	26	0.06
2	20.6	(1.4)	(−3)	1.09	27.4	26	0.06
3	18.4	(1.4)	(−4)	1.05	24.4	26	0.06
4	16.3	(1.4)	(−4)	1.03	21.6	26	0.07
5	14.3	(1.4)	(−4)	1.02	19.0	26	0.08

ical, retrieved N, q_i, and r_{ei} can be reasonable such as shown in Table 2.

As mentioned before, the optical thickness computed from retrieved values for 3 December 1997 is greater than the optical thickness that would provide the observed surface irradiance. Based on the error analysis, possible reasons for this difference besides inhomogeneity of the cloud are that 1) estimated median radii are smaller than actual median radii especially where reflectivity factors are large so that right side of (33) is positive and 2) radar calibration is off so that actual reflectivity factors are higher than the measured values or the liquid water path estimated from the microwave radiometer is less than the actual value.

5. Conclusions

This paper demonstrates that number concentration and vertical profiles of liquid water content and effective radius can be retrieved using liquid water path estimates and vertical profiles of radar reflectivity factor and Doppler velocity. An important feature of the proposed retrieval is that the height dependence of the median radius r_{ni} of the cloud particle size distribution is estimated from vertical Doppler velocity measurements obtained by a 35-GHz cloud radar. In particular, the median radius is estimated from the variance of the vertical Doppler velocity measurements using the statistical model of Considine and Curry (1996). The Considine and Curry (1996) model assumes that the distribution of vertical velocities at a given height is Gaussian with a mean of zero and that the variance of the vertical velocity uniquely determines the median radius of the cloud particles. Moreover, the model implies that the cloud particle median radius is proportional to the fourth root of the vertical velocity variance if we neglect the radius of cloud particles in a parcel of zero vertical velocity. The proposed algorithm assumes that the cloud particle number concentration is constant with height.

We used two case study periods to evaluate the algorithm, a 1.5-h period on 30 April 1994 for which we have corroborating aircraft data, and an 8.0-h period on

TABLE 2. Sensitivity to instrumental errors. Numbers in parenthesis indicate the assumed values or inputs. A minus sign (−) indicates that the retrieved value is an imaginary number.

Layer	r_n (μm)	σ_g	Z (dBZ)	q (g m^{-3})	r_e (μm)	N (cm^{-3})	β (m^{-1})
Cases 1, 2, 3 cloud, truth							
1	7.0	1.1	−24	0.60	7.2	400	0.13
2	8.0	1.1	−21	0.89	8.2	400	0.16
3	7.0	1.1	−24	0.60	7.2	400	0.13
4	6.0	1.1	−28	0.38	6.5	400	0.10
5	5.0	1.1	−33	0.22	5.4	400	0.07
Case 1 cloud, proposed retrieval, attenuated Z							
1	(7.0)	—	(−26)	0.57	6.7	460	0.13
2	(8.0)	—	(−22)	0.88	7.8	460	0.17
3	(7.0)	—	(−25)	0.61	7.0	460	0.13
4	(6.0)	1.1	(−29)	0.39	6.1	460	0.10
5	(5.0)	1.1	(−33)	0.23	5.2	460	0.07
Case 1 cloud, Frisch et al. (1995) retrieval, attenuated Z							
1	6.6	(1.1)	(−26)	0.55	6.7	480	0.12
2	7.5	(1.1)	(−22)	0.87	7.7	480	0.17
3	6.6	(1.1)	(−25)	0.61	6.7	480	0.14
4	5.6	(1.1)	(−29)	0.41	5.7	480	0.11
5	4.7	(1.1)	(−33)	0.25	4.8	480	0.08
Case 2 cloud, proposed retrieval, bias in Z							
1	(7.0)	—	(−27)	0.60	6.4	527	0.14
2	(8.0)	—	(−24)	0.89	7.3	527	0.18
3	(7.0)	—	(−27)	0.60	6.4	527	0.14
4	(6.0)	—	(−31)	0.38	5.5	527	0.10
5	(5.0)	—	(−36)	0.22	4.6	527	0.07
Case 2 cloud, Frisch et al. (1995) retrieval, bias in Z							
1	5.7	(1.1)	(−27)	0.60	5.8	724	0.15
2	6.6	(1.1)	(−24)	0.89	6.7	724	0.20
3	5.7	(1.1)	(−27)	0.60	5.9	724	0.15
4	4.9	(1.1)	(−31)	0.38	5.0	724	0.11
5	4.1	(1.1)	(−36)	0.22	4.2	724	0.08
Case 3 cloud, proposed retrieval, increased liquid water path							
1	(7.0)	1.1	(−24)	0.66	7.3	476	0.14
2	(8.0)	1.1	(−21)	0.98	8.3	476	0.18
3	(7.0)	1.1	(−24)	0.66	7.3	476	0.14
4	(6.0)	1.1	(−28)	0.41	6.2	476	0.10
5	(5.0)	1.1	(−33)	0.24	5.2	476	0.07
Case 3 cloud, Frisch et al. (1995) retrieval, increased liquid water path							
1	6.8	(1.1)	(−24)	0.66	6.9	439	0.14
2	7.8	(1.1)	(−21)	0.98	7.9	439	0.19
3	6.8	(1.1)	(−24)	0.66	6.9	439	0.14
4	5.8	(1.1)	(−28)	0.41	6.0	439	0.10
5	4.8	(1.1)	(−33)	0.24	5.0	439	0.07

3 December 1997. For the stratus case on 30 April the retrieved number concentration was 338 cm^{-3}, while in situ FSSP measurements reported a concentration of 345 cm^{-3} (Sassen et al. 1999). The retrieved and in situ average volume radii were also consistent with each other for this case.

Error analyses suggest that the error in the liquid water content vanishes and the magnitudes of the fractional error in the effective radius and shortwave extinction coefficient computed from retrieved cloud particle size distributions are half of the magnitudes of the fractional error in the estimated cloud particle median radius if the fractional error in the median radius is constant with height. Moreover, the algorithm is affected less by instrumental errors and the assumption of a lognormal distribution when the actual cloud particle size distribution deviates from lognormal as compared with algorithms that assume a prespecified value for σ_g.

Acknowledgments. We thank M. Poellot and Z. Wang for supplying processed FSSP data; Y. X. Hu, L. Smith, B. Lin and M. Ovtchinnikov for useful discussions; L. M. Hinkelman and X. Dong for useful comments; J. H. Mather for developing a delta four-stream model; and E. J. Mlawer for supplying the longwave *k*-distribution model. Data were obtained from the Atmospheric Radiation Measurement (ARM) Program sponsored by the U.S. Department of Energy, Office of Energy Research,

Office of Health and Environmental Research, Environmental Sciences Division. S. Kato was supported by the NASA Clouds and the Earth's Radiant Energy System Grant NAG-1-1963. E. Clothiaux received support for this research from the Environmental Science Division of the U.S. Department of Energy (under Grant DE-FG02-90ER61071).

APPENDIX

Median Radius Estimate from Vertical Velocity Variance

Following Considine and Curry (1996), we assume that vertical velocities w inside clouds at a given height follows a Gaussian distribution

$$P(w) = \frac{1}{(2\pi\overline{ww})^{1/2}} \exp\left(\frac{-w^2}{2\overline{ww}}\right), \tag{A1}$$

where $\overline{ww}$ is the variance of the vertical velocity. This distribution is applied to a time period, or horizontal scale, over which the mean vertical velocity is zero. Considine and Curry (1996) show that the particle radius in an adiabatically ascending or descending parcel is expressed as a function of its vertical velocity w as

$$r^2 = r_0^2 + \frac{2wKT}{g(F_K + F_D)X}, \tag{A2}$$

where

$$K = \frac{pc_p}{\epsilon L_v e_s(T)} + \frac{\epsilon L_v}{RT^2}, \tag{A3}$$

$$F_K = \left(\frac{\epsilon L_v}{RT} - 1\right)\frac{L_v\rho_w}{k_K T}, \tag{A4}$$

$$F_D = \frac{\rho_w RT}{\epsilon k_D e_s(T)}, \quad \text{and} \tag{A5}$$

$$X = \frac{\Gamma_e - \Gamma_p}{\Gamma_p - \Gamma_m}. \tag{A6}$$

In these equations g is the acceleration due to gravity, p is the total atmospheric pressure, c_p is the specific heat capacity of dry air at constant pressure, L_v is the latent heat of vaporization of water, T is the temperature of air in the parcel, $e_s(T)$ is the saturation vapor pressure at temperature T, R is the gas constant of dry air, ϵ is the ratio of the molecular weight of water to the apparent molecular weight of dry air (0.622), k_K is the thermal conductivity of air, k_D is the diffusion coefficient of water vapor in air, and ρ_w is the density of liquid water. The parameters Γ_e, Γ_p, and Γ_m represent the environment, parcel, and moist adiabatic lapse rates, respectively. The parameter X is determined by the differences between ascending or descending parcel lapse rates and the moist adiabatic and environment lapse rates. Finally, r_0 is the radius of the particles in a parcel for which the vertical velocity is zero.

Assuming that the distribution of cloud particle radii are related to the distribution of vertical velocities as

$$P(r) = P(w)\frac{dw}{dr}, \tag{A7}$$

the probability distribution of cloud particle radii becomes

$$P(r) = \frac{rD}{\sqrt{2\pi}} \exp\left[\frac{-D^2(r^2 - r_0^2)^2}{8}\right], \tag{A8}$$

where

$$D = \frac{F_K + F_D}{\overline{ww}^{1/2}}\left(\frac{gX}{KT}\right). \tag{A9}$$

In order to find the median radius of this distribution we define the cumulative distribution, $F(r)$, such that

$$F(r) = \frac{\int_0^r P(r')\,dr'}{\int_0^\infty P(r')\,dr'}. \tag{A10}$$

Since $r > 0$, if we let $\eta = [D(r^2 - r_0^2)/2\sqrt{2}]$, (A10) can be integrated to yield

$$F(r) = \frac{\operatorname{erf}\left(\frac{Dr_0^2}{2\sqrt{2}}\right) + \operatorname{erf}\left[\frac{D(r^2 - r_0^2)}{2\sqrt{2}}\right]}{\operatorname{erf}\left(\frac{Dr_0^2}{2\sqrt{2}}\right) + 1}, \tag{A11}$$

where the error function erf z is defined as

$$\operatorname{erf} z = \frac{2}{\sqrt{\pi}}\int_0^z e^{-t^2}\,dt. \tag{A12}$$

Since erf(0) = 0 and erf(0.48) $\approx$ 0.5, the median radius is

$$r_n = \left(\frac{0.96\sqrt{2}}{D}\right)^{1/2}, \tag{A13}$$

if r_0 is set to 0. Considine and Curry (1996) assume that the vertical velocity of a parcel is zero at the lifting condensation level of the parcel, which is equivalent to assuming that particles have zero radius at the lifting condensation level. The median radius as a function of $\overline{ww}$ computed by (A11) for different r_0 and X is shown in Fig. A1. Here $F_K + F_D$ to compute D by (A9) is set to 1.47×10^{10} s m^{-2} (Rogers and Yau 1989, p. 104). The median radius is not a strong function of r_0 for r_0 smaller than 5 μm except for small $\overline{ww}$. When X increases, which means the lapse rate of the parcel approaches the moist adiabatic lapse rate, (A2) shows that the median radius becomes less dependent on $\overline{ww}$.

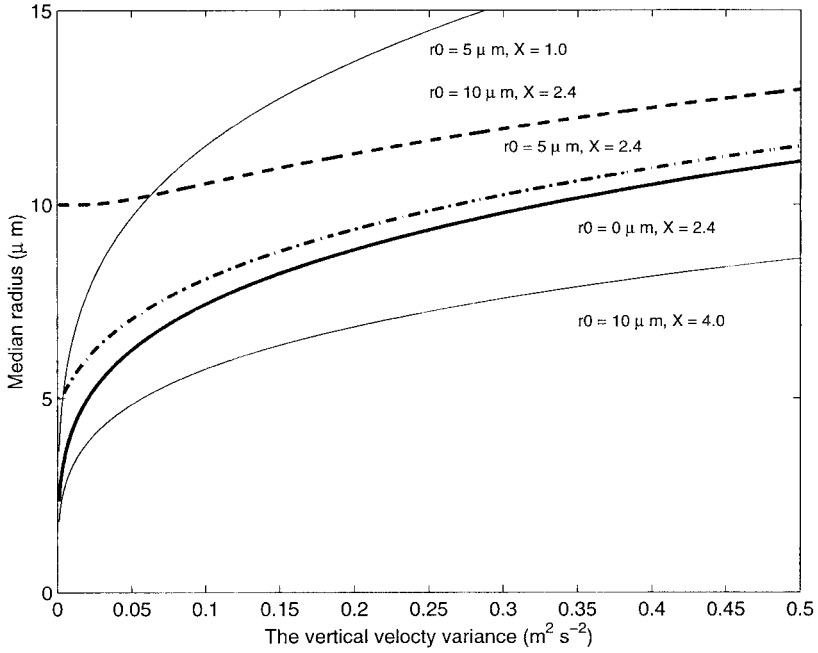

FIG. A1. Median radius as a function of the vertical velocity variance for different r_0 and X computed by (A11).

REFERENCES

Albrecht, B. A., R. S. Penc, and W. H. Schubert, 1985: An observational study of cloud-topped mixed layers. *J. Atmos. Sci.,* **42,** 800–822.

——, C. W. Fairall, D. W. Thomson, and A. B. White, 1990: Surface-based remote sensing of the observed and the adiabatic liquid water content of stratocumulus clouds. *Geophys. Res. Lett.,* **17,** 89–92.

Clothiaux, E. E., M. A. Miller, B. A. Albrecht, T. P. Ackerman, J. Verlinde, D. M. Babb, R. M. Peters, and W. J. Syrett, 1995: An evaluation of a 94-GHz radar for remote sensing of cloud properties. *J. Atmos. Oceanic Technol.,* **12,** 201–229.

——, T. P. Ackerman, G. G. Mace, K. P. Moran, R. T. Marchand, M. A. Miller, and B. E. Martner, 2000: Objective determination of cloud heights and radar reflectivities using a combination of active remote sensors at the ARM CART sites. *J. Appl. Meteor.,* **39,** 645–665.

Considine, G., and J. A. Curry, 1996: A statistical model of drop-size spectra for stratocumulus clouds. *Quart. J. Roy. Meteor. Soc.,* **122,** 611–634.

Dong, X., P. Minnis, T. P. Ackerman, E. E. Clothiaux, G. G. Mace, C. N. Long, and J. C. Lijegren, 2000: A 25-month database of stratus cloud properties generated from ground-based measurements at the Atmospheric Radiation Measurement Southern Great Plains site. *J. Geophys. Res.,* **105,** 4529–4537.

Ellingson, R. G., J. Ellis, and S. Fels, 1991: The intercomparison of radiation codes used in climate models: Long-wave results. *J. Geophys. Res.,* **96,** 8929–8953.

Frisch, A. S., C. W. Fairall, and J. B. Snider, 1995: Measurement of stratus cloud and drizzle parameters in ASTEX with a K_α-band Doppler radar and a microwave radiometer. *J. Atmos. Sci.,* **52,** 2788–2799.

——, G. Feingold, C. W. Fairall, T. Uttal, and J. B. Snider, 1998: On cloud radar and microwave radiometer measurements of stratus cloud liquid water profiles. *J. Geophys. Res.,* **103,** 23 195–23 197.

Fu, Q., K.-N. Liou, M. C. Cribb, T. P. Charlock, and A. Grossman, 1997: Multiple scattering parameterization in thermal infrared radiative transfer. *J. Atmos. Sci.,* **54,** 2799–2812.

Hansen, J. E., and L. D. Travis, 1974: Light scattering in planetary atmospheres. *Space Sci. Rev.,* **16,** 527–610.

Hinds, W. C., 1982: *Aerosol Technology; Properties, Behavior, and Measurement of Air-borne Particles.* John Wiley and Sons, 504 pp.

Hu, Y. X., and K. Stamnes, 1993: An accurate parameterization of the radiative properties of water clouds suitable for use in climate models. *J. Climate,* **6,** 728–742.

Kato, S., T. P. Ackerman, J. H. Mather, and E. E. Clothiaux, 1999: The *k*-distribution method and correlated-*k* approximation for a shortwave radiative transfer model. *J. Quant. Spectrosc. Radiat. Transfer,* **62,** 109–121.

Khairroutdinov, M. F., and Y. L. Kogan, 1999: A large eddy simulation model with explicit microphysics: Validation against aircraft observations of a stratocumulus-topped boundary layer. *J. Atmos. Sci.,* **56,** 2115–2131.

Liljegren, J. C., 1995: Observations of total column precipitable water vapor and cloud liquid water using a dual-frequency microwave radiometer. *Microwave Radiometry and Remote Sensing of the Environment,* D. Solimini, Ed., VSP Press, 107–118.

Liou, K.-N., Q. Fu, and T. P. Ackerman, 1988: A simple formulation of the delta-four-stream approximation for radiative transfer parameterizations. *J. Atmos. Sci.,* **45,** 1940–1947.

Mace, G. G., and K. Sassen, 2000: A constrained algorithm for retrieval of stratocumulus cloud properties using solar radiation, microwave radiometer, and millimeter cloud radar data. *J. Geophys. Res.,* **105,** 29 099–29 108.

Mason, B. J., and C. W. Chien, 1962: Cloud-droplet growth by condensation in cumulus. *Quart. J. Roy. Meteor. Soc.,* **88,** 136–142.

Miles, N. L., J. Verlinde, and E. E. Clothiaux, 2000: Cloud droplet size distributions in low-level stratiform clouds. *J. Atmos. Sci.,* **57,** 295–311.

Mlawer, E. J., S. J. Taubman, P. D. Brown, M. J. Iacono, and S. A. Clough, 1997: Radiative transfer for inhomogeneous atmosphere: RRTM, a validated correlated-*k* model for the longwave. *J. Geophys. Res.,* **102,** 16 663–16 682.

Moran, K. P., B. E. Martner, M. J. Post, R. A. Kropfli, D. C. Welsh, and K. B. Widene, 1998: An unattended cloud-profiling radar

for use in climate research. *Bull. Amer. Meteor. Soc.,* **79,** 443–455.
Nicholls, S., 1984: The dynamics of stratocumulus: Aircraft observations and comparisons with a mixed layer model. *Quart. J. Roy. Meteor. Soc.,* **110,** 783–820.
Noonkester, V. R., 1984: Droplet spectra observed in marine stratus cloud layers. *J. Atmos. Sci.,* **41,** 829–845.
Ovtchinnikov, M., and Y. L. Kogan, 2000: Evaluation of radar retrieval algorithms in stratiform clouds using large-eddy simulations. *J. Geophys. Res.,* **105,** 17 351–17 359.
Rogers, R. R., and M. K. Yau, 1989: *A Short Course in Cloud Physics.* Pergamon Press, 293 pp.
Sassen, K., G. G. Mace, Z. Wang, M. R. Poellot, S. M. Sekelsky, and R. E. Mcintosh, 1999: Continental stratus clouds: A case study using coordinated remote sensing and aircraft measurements. *J. Atmos. Sci.,* **56,** 2345–2358.
Stephens, G. L., and C. M. R. Platt, 1987: Aircraft observations of the radiative and microphysical properties of stratuscumulus and cumulus cloud fields. *J. Climate Appl. Meteor.,* **26,** 1243–1269.
Stokes, G. M., and S. E. Schwartz, 1994: The Atmospheric Radiation Measurement (ARM) Program: Programmatic background and design of the Cloud and Radiation Test Bed. *Bull. Amer. Meteor. Soc.,* **75,** 1201–1221.
Toon, O. B., C. P. Mckay, and T. P. Ackerman, 1989: Rapid calculation of radiative heating rates and photodissociation rates in inhomogeneous multiple scattering atmosphere. *J. Geophys. Res.,* **94,** 16 287–16 301.
Twomey, S., and C. F. Bohren, 1980: Simple approximations for calculation of absorption in clouds. *J. Atmos. Sci.,* **37,** 2086–2094.
White, A. B., C. W. Fairall, and D. W. Thomson, 1991: Radar observations of humidity variability in and above the marine atmospheric boundary layer. *J. Atmos. Oceanic Technol.,* **8,** 639–658.
Wiscombe, W. J., R. M. Welch, and W. D. Hall, 1984: The effects of very large drops on cloud absorption. Part I: Parcel models. *J. Atmos. Sci.,* **41,** 1336–1355.